Available online at www.sciencedirect.com
SCIENCE DIRECT®
Journal of Photochemistry and Photobiology A: Chemistry 157 (2003) 161–166
Journal of Photochemistry and Photobiology A:Chemistry
www.elsevier.com/locate/jphotochem

Gas phase UV absorption spectra for peracetic acid, and for acetic acid monomers and dimers

John J. Orlando*, Geoffrey S. Tyndall

Atmospheric Chemistry Division, National Center for Atmospheric Research, P.O. Box 3000 Boulder, CO 80307, USA

Received 24 April 2002; received in revised form 14 September 2002; accepted 14 September 2002

Abstract

Absorption cross sections have been determined in the UV spectral region (205–350 nm) for gas phase acetic acid ($CH_3C(O)OH$) in its monomeric and dimeric forms (270–345 K), as well as for peracetic acid ($CH_3C(O)OOH$, 248 and 298 K). Analysis of acetic acid spectra recorded over a range of pressures (0.12–3.6 Torr), coupled with a prior knowledge of the dimerization equilibrium constant, allowed for the deconvolution of the monomer and dimer absorption spectra. The 298 K monomer spectrum consists of a maximum near 207 nm ($\sigma = 1.4 \times 10^{-19}$ cm^2 per molecule), with monotonically decreasing cross sections at longer wavelengths. The dimer spectrum possesses a maximum located short of 205 nm, with a peak intensity about double that of the monomer. The first gas phase spectrum of peracetic acid is also reported, which is similar to a previously published solution-phase spectrum. Measurable absorption extends to 340 nm at 298 K, and it is determined that the tropospheric photolysis of this species will be a reasonably rapid process (lifetime ≈ weeks), which will play at least a minor role in its atmospheric destruction.

Keywords: Gas phase UV absorption; Peracetic acid; Acetic acid

1. Introduction

The oxidation of hydrocarbon species (both man-made and natural) in the earth's lower atmosphere leads to the generation of a number of secondary pollutants, including ozone and a multitude of partially oxidized oxygen- and nitrogen-containing organic species [1–3]. Among this mix of organic species are the carboxylic and peroxycarboxylic acids, which are believed to be derived largely from the reactions of HO_2 radicals with peroxyacyl species [4–7], e.g.:

$$CH_3C(O)O_2 + HO_2 \rightarrow CH_3C(O)OOH + O_2 \quad \text{(R1a)}$$

$$CH_3C(O)O_2 + HO_2 \rightarrow CH_3C(O)OH + O_3 \quad \text{(R1b)}$$

The peroxyacyl radicals are generated either from the oxidation of aldehydes:

$$OH + CH_3CHO \rightarrow CH_3C(O) + H_2O \quad \text{(R2)}$$

$$CH_3C(O) + O_2 + M \rightarrow CH_3C(O)O_2 + M \quad \text{(R3)}$$

or from the decomposition of radicals generated in the oxidation of larger species, for example, acetone [8,9]:

$$OH + CH_3C(O)CH_3(+O_2) \rightarrow CH_3C(O)CH_2O_2 + H_2O \quad \text{(R4)}$$

$$CH_3C(O)CH_2O_2 + NO \rightarrow CH_3C(O) + CH_2O + NO_2 \quad \text{(R5)}$$

$$CH_3C(O) + O_2 + M \rightarrow CH_3C(O)O_2 + M \quad \text{(R3)}$$

Although the production of peracetic acid, $CH_3C(O)OOH$, in reaction (1) has clearly been shown in the laboratory [4,5,7], no measurements of its atmospheric abundance have yet been made. On the other hand, acetic acid has been detected in the gas phase and has also been shown to be a ubiquitous component of rainwater (e.g. [10–17]). Atmospheric loss processes for these species (particularly peracetic acid) have yet to be firmly established. Heterogeneous processes (i.e. wet and dry deposition) will likely play a role, as will reaction with OH [18]. While acetic acid possesses no measurable absorption in the actinic region of the spectrum ($\lambda > 290$ nm) [19] and thus will not be subject to photolytic destruction in the troposphere, no gas phase UV absorption spectra for peracetic acid have been reported to date.

* Corresponding author. Tel.: +1-303-497-1486; fax: +1-303-497-1411.
E-mail address: orlando@ucar.edu (J.J. Orlando).

1010-6030/03/$ – see front matter © 2003 Elsevier Science B.V. All rights reserved.
doi:10.1016/S1010-6030(03)00067-4

In this work, the first gas phase spectrum of peracetic acid is reported over the range 200–350 nm. Since acetic acid is found as an impurity in the peracetic acid samples used, its spectrum was also studied in the same wavelength region. Measurements were made over a range of pressures, allowing for the deconvolution of the acetic acid monomer and dimer spectra. Comparisons are made with previously reported acetic acid spectra. The impact of photolysis on the atmospheric destruction of peracetic acid is also discussed.

2. Experimental

Spectral measurements in the near UV were made using a conventional spectrometer system, which has been described previously [20,21]. Briefly, measurements were made in a 90 cm long, temperature-regulated cylindrical pyrex absorption cell, equipped with Suprasil quartz windows. Measurements were made over a range of temperatures (acetic acid at 270, 298, 325, and 345 K; peracetic acid at 248 and 298 K). The beam from a deuterium lamp is collimated, passed through the absorption cell, and is then focussed onto the entrance slit of a 0.3 m Czerny-Turner spectrograph equipped with a 300 groove mm^{-1} grating, which disperses the light onto a 1024-pixel diode array detector (EG&G Model 1420). Under this configuration, the spectral resolution of the spectrometer system is 0.6 nm with each pixel separated in wavelength by about 0.25 nm. Wavelength calibrations were done via interpolation between the positions of the emission lines of a low pressure mercury lamp. Spectra were typically obtained via the summation of 100 exposures of the diode array, each of 0.2 s duration. Raw spectral data at each pixel, $I(\lambda)$, were converted to absorbance units (base e) via comparison with a reference spectrum, $I_o(\lambda)$, recorded with the absorption cell evacuated:

$$A(\lambda) = \ln\left\{\frac{I_o(\lambda)}{I(\lambda)}\right\} \quad \text{(A)}$$

Absorption spectra were then smoothed and the smoothed data interpolated to obtain absorbance values at 0.5 nm intervals.

For measurements of gas phase acetic acid (monomer and dimer) spectra, vapors above a sample of glacial acetic acid (99.8%, Aldrich) were added to the absorption cell using a standard vacuum system. The glacial acetic acid sample was first degassed via repetitive freeze–pump–thaw cycles. Spectra were obtained at pressures ranging from 0.12 to 3.6 Torr. Determination of the monomer and dimer absorption cross sections from the measured spectra required a complex deconvolution procedure. This procedure, and the uncertainties in the resulting data, are described in the results section.

Peracetic acid was purchased from Aldrich (32 wt.% in dilute aqueous acetic acid solution). Before use, the sample was pumped on for a few hours to approximately 20% of its initial volume to remove the majority of the water. Contents of the vapors above the remaining sample were analyzed by FTIR spectroscopy [9] to determine the level of water and acetic acid impurity; typically, these vapors were found to contain about 60–70% peracetic acid, with the remainder being acetic acid and water (each ≈15%). The same sample was then used to make a series of UV measurements, with total sample pressure varied over the range 0.08 to 1.0 Torr. IR absorption measurements conducted before and after the UV measurements showed no measurable change in the sample purity. H_2O_2, a potential impurity in the peracetic acid samples, is known to be rapidly converted to H_2O in both our IR and UV absorption cells, and thus is unlikely to make any contribution to the spectral measurements.

UV absorption cross sections were obtained in conventional fashion using Beer's law:

$$A(\lambda) = \sigma(\lambda) l c \quad \text{(B)}$$

Cross sections were obtained from the slope of plots of A/l versus concentration at each wavelength (where l is the absorption pathlength, c is the peracetic acid concentration, and σ is the absorption cross section). Concentrations used in the analysis were corrected for the presence of H_2O and acetic acid impurity (as determined from the infrared spectra), and measured absorbances were corrected for a minor (<5%) spectral contribution from acetic acid monomer and dimer.

3. Results and discussion

3.1. Acetic acid

The dimerization of acetic acid is a well characterized process, with the recommended value for the dimerization equilibrium constant given as follows [4,22]: $K_{eq} = P_D/P_M^2 = 7.1 \times 10^{-9} \exp(7705/T)$, for dimer ($P_D$) and monomer ($P_M$) partial pressures given in units of atm. Thus, under the conditions of our experiments, measured absorbance spectra will contain contributions from both the monomer and the dimer:

$$\frac{A(\lambda)}{l} = \sigma_M(\lambda)[M] + \sigma_D(\lambda)[D] \quad \text{(C)}$$

where $A(\lambda)$ is the measured absorbance at wavelength λ, l is the absorption pathlength, $\sigma_M(\lambda)$ and $\sigma_D(\lambda)$ are the absorption cross sections for the monomer and dimer at wavelength λ, and [M] and [D] are the concentrations of the monomer and dimer in units of molecule cm^{-3}, respectively.

Absorption cross sections for the acetic acid monomer and dimer were obtained as follows. First, composite spectra were obtained at a number of different total pressures (ranging from 0.12 to 3.6 Torr at 298 K and above, and from 0.15 to 1.5 Torr at 270 K). Concentrations for the monomer and dimer were then calculated for each pressure using K_{eq} given above, and a series of equations of the form (C) was thus created for each wavelength interval (i.e. each 0.5 nm) in which the only unknowns are the monomer and dimer cross sections, $\sigma_M(\lambda)$ and $\sigma_D(\lambda)$. Cross sections for both the

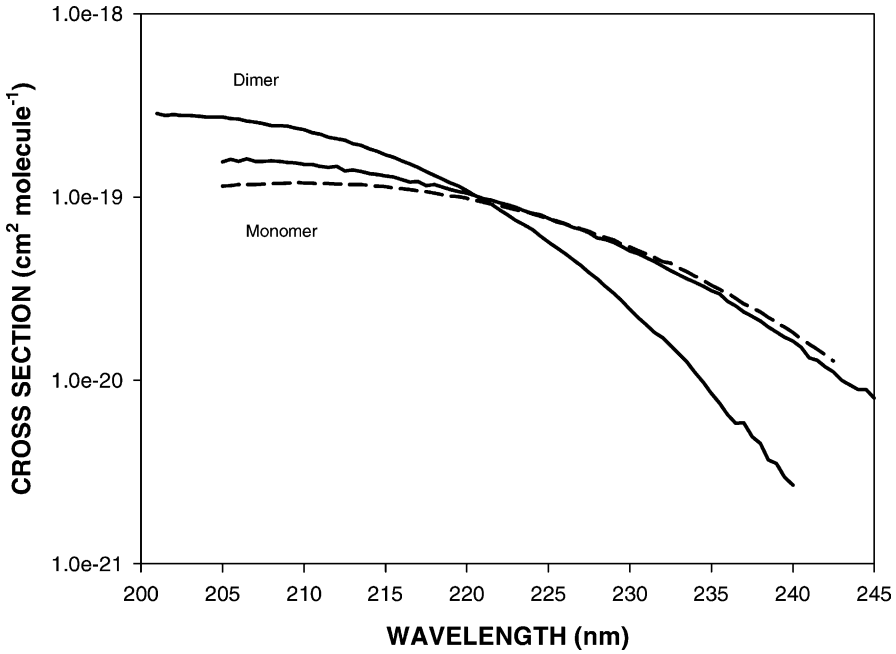

Fig. 1. Gas phase acetic acid (monomer and dimer) spectra obtained in this work. Solid lines, 298 K spectra; dashed line, acetic acid spectrum at 345 K.

monomer and dimer were then obtained at each wavelength from a least-squares fitting procedure, in which $\sigma_M(\lambda)$ and $\sigma_D(\lambda)$ were varied to achieve best agreement between measured and calculated (Eq. (C)) values of $A(\lambda)$.

Uncertainties in the acetic acid cross section data arise from errors in absorbance, pathlength, and pressure, and also from uncertainty in the dimerization equilibrium constant, in the measurement of temperature (which impacts the equilibrium), and in the fitting procedure. Estimated uncertainties for the monomer cross sections are ±15% below 220 nm, and ±35% near 240 nm. Uncertainties in the dimer cross sections are probably slightly higher, ±25% below 220 nm and ±50% near 235 nm.

Room temperature spectra for the monomer and dimer obtained via this fitting procedure are shown as the solid lines in Fig. 1. The cross section data are also given at 2 nm intervals in Table 1. The analysis clearly shows that the two spectra differ from each other in both shape and intensity. The monomer spectrum displays a broad maximum near 207 nm, with σ_M (207 nm) = $(1.5 \pm 0.2) \times 10^{-19}$ cm^2 per molecule, and monotonically decreases in intensity with increasing wavelength. The absorption maximum for the dimer, on the other hand, appears at shorter wavelength ($\lambda_{max} < 205$ nm), and is about twice as intense as the monomer, σ_D(205 nm) = $(2.5 \pm 0.5) \times 10^{-19}$ cm^2 per molecule. The decrease in cross section with increasing wavelength is more rapid for the dimer than for the monomer, resulting in higher values of $\sigma_M(\lambda)$ than $\sigma_D(\lambda)$ at $\lambda > 225$ nm.

Analogous sets of measurements were taken at 270, 325, and 345 K. Measurements at lower temperatures were not possible, due to the low vapor pressure of the acetic acid samples. As an example, the spectrum of the monomer obtained at 345 K is shown as the dashed line in Fig. 1. The monomer spectrum appears to be slightly broader at higher temperature (lower cross section near the peak, higher at longer wavelengths compared to the 298 K spectrum), though the observed changes over the full range of temperatures examined are probably comparable in magnitude to the uncertainty in the measurements. The retrieved dimer spectra at different temperatures showed no discernible trend with temperature; cross sections obtained near the peak of the spectrum varied by about ±10% from temperature to

Table 1
Gas phase UV absorption cross sections for acetic acid monomer and dimer at 298 K, at 2 nm intervals

Wavelength (nm)	Monomer cross section (10^{-21} cm^2 per molecule)	Dimer cross section (10^{-21} cm^2 per molecule)
210	151	234
212	147	209
214	135	184
216	125	158
218	117	132
220	105	109
222	93.3	85.4
224	81.9	66.8
226	71.7	49.5
228	60.0	36.0
230	50.9	24.5
232	42.0	17.1
234	34.4	11.1
236	27.1	6.5
238	21.1	4.5
240	16.4	2.7
242	11.9	
244	8.9	

temperature, while the scatter was of order ±40% at 240 nm. As discussed above, this scatter is likely due to uncertainties inherent to the measurement of temperature and in the analysis procedure.

Comparisons of our data with previous work [19,23–25] are difficult to do in most cases, as quantitative accounting for the presence of both the monomer and dimer were seldom carried out and insufficient details are given to assess the relative dimer and monomer contributions to the measured spectra. In fact, other than a single wavelength determination by Singleton et al. [25], absorption cross sections for the dimer have not been previously reported. Singleton et al. [25] used a procedure similar to ours to obtain monomer and dimer absorption cross sections at 222 nm; their data are in reasonable agreement with ours (their monomer value is about 25% lower and their dimer value about 15% higher than our values). Spectra reported by both Calvert and Pitts [19] and by Suto et al. [24] possess shapes similar to that of the dimer, but with cross sections similar in magnitude to the monomer at short wavelength (see Fig. 1). Both of these studies indicate the likelihood of contribution to the spectrum from the dimer, but insufficient details are given to make any quantitative assessment. The liquid phase acetic acid spectrum of Giguère and Olmos [26], reported over the range 225–245 nm, also resembles more closely that of the dimer than that of the monomer. The spectrum reported by Barnes et al. [23], attributed to the monomer, is very similar in shape and magnitude to our monomer spectrum. As alluded to in the introduction, the lack of any significant absorption in the near UV portion of the spectrum (i.e. in the actinic region beyond 290 nm) means that photolysis will not contribute to the tropospheric destruction of acetic acid.

3.2. Peracetic acid

The peracetic acid UV absorption spectrum (298 K, 205–340 nm), obtained using a conventional Beer's law analysis (see Section 2), is shown in Fig. 2. Cross sections are given at 2 nm intervals in Table 2. At short wavelengths, uncertainties in the peracetic acid cross section data are dominated by the uncertainty in the peracetic acid concentration determination (±10%), with minor (±1%) contributions from errors in the measurement of absorbance, pressure and pathlength. At longer wavelengths, relative uncertainties in the absorbance measurement increase as the cross sections decrease. Overall, estimated uncertainties range from ±10% at $\lambda < 290$ nm, to ±20% at 320 nm, and about ±50% at 330 nm.

Absorption cross sections are seen to decrease in a monotonic, pseudo-exponential fashion over the range measured, decreasing from a value near 10^{-18} cm^2 per molecule at 205 nm to about 10^{-22} cm^2 per molecule at 340 nm. Though measurements are difficult to make at low temperature due to the reduced vapor pressure, the 248 K spectrum shows an apparently faster fall-off with wavelength than was the case at 298 K.

To the best of our knowledge, the gas phase peracetic acid absorption spectrum has not been previously measured. However, Giguère and Olmos [26] have reported peracetic acid spectra in both aqueous and isooctane solution, which

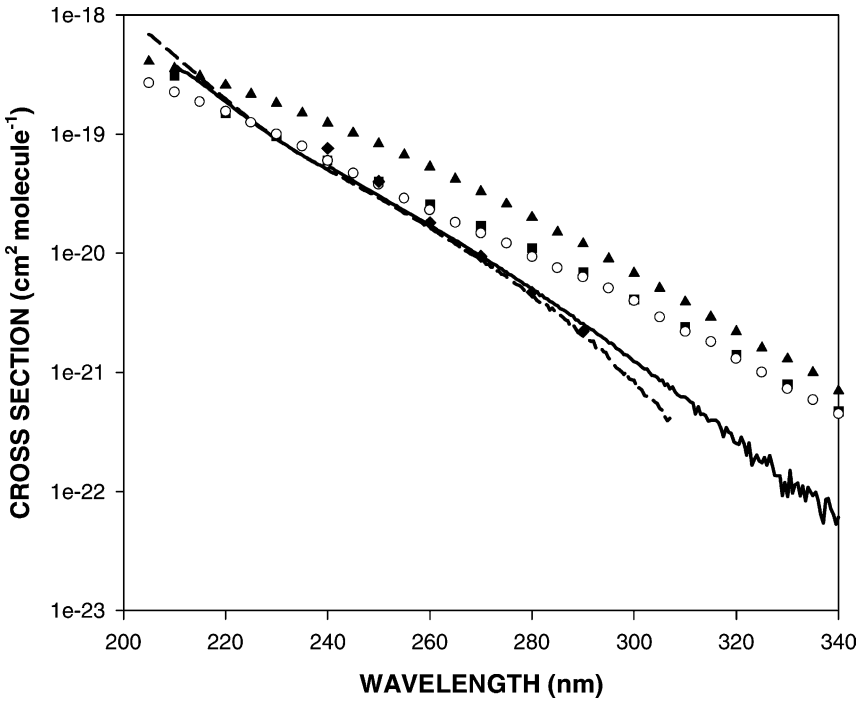

Fig. 2. Gas phase peracetic acid spectra at 298 K (solid line, this work) and 248 K (dashed line, this work). Other data shown are for peracetic acid in isooctane solution (diamonds [26]), gas phase H_2O_2 (triangles [18]), CH_3OOH (squares [18]), and $HOCH_2OOH$ (open circles [27]).

Table 2
UV absorption cross sections for peracetic acid in the gas phase, at 2 nm intervals

Wavelength (nm)	Cross section (10^{-21} cm^2 per molecule)
210	381
212	331
214	295
216	254
218	217
220	189
222	160
224	139
226	120
228	105
230	91.0
232	80.1
234	70.3
236	63.1
238	56.1
240	50.3
242	48.3
244	43.1
246	38.2
248	34.1
250	30.5
252	27.1
254	24.2
256	21.6
258	19.3
260	17.1
262	15.3
264	13.5
266	12.1
268	10.6
270	9.45
272	8.35
274	7.42
276	6.51
278	5.74
280	5.06
282	4.44
284	3.86
286	3.34
288	2.97
290	2.56
292	2.26
294	1.93
296	1.70
298	1.41
300	1.23
302	1.07
304	0.94
306	0.78
308	0.69
310	0.62
312	0.45
314	0.44
316	0.40
318	0.35
320	0.25
322	0.20
324	0.20
326	0.17
328	0.14
330	0.09
332	0.11
334	0.11
336	0.09
338	0.09
340	0.06

appear very similar to each other and to our data (see Fig. 2). The peracetic acid spectrum also bears a resemblance to those of other peroxides (H_2O_2, CH_3OOH, and $HOCH_2OOH$) for which data are available [18,27], though the peracetic acid spectrum is weaker and falls off more steeply with wavelength than do the spectra of these other species.

Possible tropospheric removal processes for gas phase peracetic acid include photolysis, reaction with OH, and removal by heterogeneous processes (wet and dry deposition). Using the absorption cross sections obtained herein, tabulated solar flux data [28], and assuming a photodissociation quantum yield of unity, the peracetic acid photolysis lifetime is estimated to be about 3–4 weeks, for typical mid-latitude summer conditions, roughly independent of altitude. The rate coefficient for reaction of OH with peracetic acid has not been measured but, by analogy to the reactivity of OH with H_2O_2 and CH_3OOH [18], a value on the order of $(1–5) \times 10^{-12}$ cm^3 per molecule s^{-1} seems plausible, which would imply a peracetic acid lifetime against OH reaction of about 2–12 days. Peracetic acid is only moderately soluble in aqueous solution, $H = 670$ M atm^{-1} [29,30] at 298 K, and hence wet and dry deposition processes [31,32] are not likely to be rapid (lifetimes of weeks or more). Thus, photolysis of peracetic acid will occur on a timescale that is comparable to other loss processes, and will play at least a minor role in its tropospheric removal. Studies of its rate coefficient with OH would clearly be useful in establishing more firmly the tropospheric lifetime of this species.

Acknowledgements

The National Center for Atmospheric Research is operated by the University Corporation for Atmospheric Research, under the sponsorship of the National Science Foundation. This work was funded in part by the NASA Upper Atmosphere Research Program. Thanks are due to Alan Fried and Mary Barth (both of NCAR) for their careful reading of the manuscript.

References

[1] G.P. Brasseur, J.J. Orlando, G.S. Tyndall (Eds.), Atmospheric Chemistry and Global Change, Oxford University Press, New York, 1999.
[2] R. Atkinson, J. Phys. Chem. Ref. Data Monogr. 2 (1997) 1.
[3] R. Atkinson, J. Phys. Chem. Ref. Data 26 (1997) 215.
[4] M.A. Crawford, T.J. Wallington, J.J. Szente, M.M. Maricq, J.S. Francisco, J. Phys. Chem. A 103 (1999) 365.
[5] H. Niki, P.D. Maker, C.M. Savage, L.P. Breitenbach, J. Phys. Chem. 89 (1985) 588.
[6] G.K. Moortgat, B. Veyret, R. Lesclaux, Chem. Phys. Lett. 160 (1989) 443.
[7] O. Horie, G.K. Moortgat, J. Chem. Soc., Faraday Trans. 88 (1992) 3305.
[8] M.E. Jenkin, R.A. Cox, M. Emrich, G.K. Moortgat, J. Chem. Soc., Faraday Trans. 89 (1993) 2983.

[9] J.J. Orlando, G.S. Tyndall, L. Vereecken, J. Peeters, J. Phys. Chem. A 104 (2000) 11578.
[10] M. Andreae, R.W. Talbot, T.W. Andreae, R.C. Harriss, J. Geophys. Res. 93 (1988) 1616.
[11] D.J. Jacob, S.C. Wofsy, J. Geophys. Res. 93 (1988) 1477.
[12] T. Reiner, O. Mohler, F. Arnold, J. Geophys. Res. 104 (1999) 13943.
[13] R.W. Talbot, M.O. Andreae, H. Berresheim, D.J. Jacob, K.M. Beecher, J. Geophys. Res. 95 (1990) 16799.
[14] G.A. Dawson, J.C. Farmer, J.L. Moyers, Geophys. Res. Lett. 7 (1980) 725.
[15] D. Grosjean, Env. Sci. Technol. 23 (1989) 1506.
[16] J.E. Lawrence, P. Koutrakis, Env. Sci. Technol. 28 (1994) 957.
[17] R.W. Talbot, et al., J. Geophys. Res. 100 (1995) 9335.
[18] W.B. DeMore, S.P. Sander, D.M. Golden, R.F. Hampson, M.J. Kurylo, C.J. Howard, A.R. Ravishankara, C.E. Kolb, M.J. Molina, Chemical kinetics and photochemical data for use in stratospheric modeling, Evaluation no. 12, NASA JPL Publication 97-4, 1997.
[19] J.G. Calvert, J.N. Pitts Jr., Photochemistry, Wiley, New York, 1966.
[20] T.A. Staffelbach, J.J. Orlando, G.S. Tyndall, J.G. Calvert, J. Geophys. Res. 100 (1995) 14189.
[21] J.J. Orlando, G.S. Tyndall, J.-M. Fracheboud, E. Estupinan, S. Haberkorn, A. Zimmer, Atmos. Environ. 33 (1999) 1621.
[22] J. Chao, B.J. Zwolinski, J. Phys. Chem. Ref. Data 7 (1978) 363.
[23] E.E. Barnes, W.T. Simpson, J. Chem. Phys. 39 (1963) 670.
[24] M. Suto, X. Wang, L.C. Lee, J. Phys. Chem. 92 (1988) 3764.
[25] D.L. Singleton, G. Paraskevopoulos, R.S. Irwin, J. Phys. Chem. 94 (1990) 695.
[26] P.A. Giguère, A.W. Olmos, Can. J. Chem. 34 (1956) 689.
[27] S. Bauerle, G.K. Moortgat, Chem. Phys. Lett. 309 (1999) 43.
[28] S. McKeen, NOAA Aeronomy Lab, personal communication (1991).
[29] J. Lind, G. Kok, J. Geophys. Res. 91 (1986) 7889.
[30] J. Lind, G. Kok, J. Geophys. Res. 99 (1994) 21119.
[31] F. Giorgi, W.L. Chameides, J. Geophys. Res. 90 (1985) 7872.
[32] M.L. Wesely, Atmos. Environ. 23 (1989) 1293.